

**JOURNAL OF THE ROYAL SOCIETY
INTERFACE****Alginate foam-based 3-D culture to investigate drug
sensitivity in primary leukaemia cells**

Journal:	<i>Journal of the Royal Society Interface</i>
Manuscript ID	rsif-2017-0928.R3
Article Type:	Research
Date Submitted by the Author:	27-Mar-2018
Complete List of Authors:	Karimpoor, Mahroo; University College London, mechanical engineering Yebra-Fernandez, Eva; Molecular Pathology, North West London Pathology, Hammersmith Hospital, London Parhizkar, Maryam; Department of Mechanical Engineering, University College London Orlu, Mine; School of Pharmacy, University College London Craig, Duncan Q. M. ; UCL School of Pharmacy, UCL School of Pharmacy Sorouri Khorashad, Jamshid; Molecular Pathology, North West London Pathology, Hammersmith Hospital, London; Centre for Haematology, Department of Medicine, Imperial College, Hammersmith Hospital Edirisinghe, Mohan; UCL, Mechanical
Categories:	Life Sciences - Engineering interface
Subject:	Biomaterials < CROSS-DISCIPLINARY SCIENCES
Keywords:	Scaffold, Leukaemia, three-dimensional, culture, drug resistance

SCHOLARONE™
Manuscripts

Alginate foam-based 3-D culture to investigate drug sensitivity in primary leukaemia cells

Mahroo Karimpoor^{1,2,3}, Eva Yebra-Fernandez⁴, Maryam Parhizkar¹, Mine Orlu³, Duncan Craig³,
Jamshid S Khorashad^{2,4} Mohan Edirisinghe¹

¹*Department of Mechanical Engineering, University College London, Torrington Place, London, WC1E 7JE, UK*

²*Centre for Haematology, Department of Medicine, Imperial College, Hammersmith Hospital, Du Cane Road, London, W12 0NN, UK*

³*School of Pharmacy, University College London, 29-39 Brunswick Square, London, WC1N 1AX, UK*

⁴*Molecular Pathology, North West London Pathology, Hammersmith Hospital, London, W12 0HS, UK*

Running heads: Porous alginate foam scaffold for antileukaemia

Correspondence:

Professor Mohan Edirisinghe

m.edirisinghe@ucl.ac.uk

409 Roberts (Engineering Building), Torrington Place, London, WC1E 7JE.

Tel: 00442076793942, Ex: 33942

Fax: 00442073880180

Abstract

Development of assays for evaluating the sensitivity of leukaemia cells to anti-cancer agents is becoming an important aspect of personalized medicine. The conventional cell cultures lack the three-dimensional (3D) structure of the bone marrow, the extracellular matrix and stromal components which are crucial for the growth and survival of leukaemia stem cells. To accurately predict the sensitivity of the leukaemia cells in an *in vitro* assay a culturing system containing the essential components of bone marrow is required. In this study, we developed a porous calcium alginate foam-based scaffold to be used for 3D culture. The new 3D culture showed to be cell compatible as it supported the proliferation of both normal hematopoietic and leukaemia cells. Our cell differential assay for myeloid markers showed that the porous foam-based 3D culture enhanced myeloid differentiation in both leukaemia and normal hematopoietic cells compared to 2D culture. The foam-based scaffold reduced the sensitivity of the leukaemia cells to the tested antileukemia agents in K562 and HL60 leukemia cell line model and also primary myeloid leukaemia cells. This observation supports the application of calcium alginate foams as scaffold component of the 3D cultures for investigation of sensitivity to antileukaemia agents in primary myeloid cells.

Key words: Scaffold; Leukaemia; three-dimensional, culture, drug resistance

1.Introduction

The bone marrow (BM) niche is a specialized microenvironment where stem cells reside. The niche is believed to regulate stem cell quiescence, self-renewal and differentiation[1]. There are several components that regulate the function of the niches [2-4]. These factors include cellular components such as osteoblast, osteoclasts, endothelial cells, mesenchymal progenitors and molecules such as stromal derived factor1 (SDF-1), stem cell factor, osteopontin, thrombopoietin and N-cadherin[5].

Traditionally monolayer cell culture has been used for studying hematopoietic stem cells (HSC) but they are not capable of producing a niche like structure and therefore have not been suitable models for this purpose[6]. Considering the deficiencies of current two-dimensional cultures[7], recent efforts has focused on developing 3D cultures which can mimic BM microenvironment by accommodating the essential components of the BM. The cultures with only cellular and cytokine components without providing the 3 dimensional structure have been able to support the expansion of the more differentiated hematopoietic precursor CD34⁺ cells without establishing a support for long-term HSC self-renewal[3]. A lack of 3D structure and molecular matrix components are potential causes of their unsustainability for long-term HSC culture[8]. Molecules present in the 3D structure have significant impact on making the culture more similar to BM niches including segment-1(CS-1) and RGD motifs which mimic the fibronectin domains of the extracellular matrix (ECM) and contribute to expansion of CD34⁺ cells[9].

The development of an *ex-vivo* 3D culture mimicking the BM microenvironment in providing niche-like structures for the HSC to reside and proliferate provides an opportunity to study hematological malignancies. The acute myeloid leukaemia (AML) cells have a subpopulation called leukaemia stem cells (LSC) which has the capacity to initiate the disease and continue producing leukaemia cells and also perform self-renewal. The main challenge for studying

1
2
3 AML cells for therapeutic target discovery purposes has been the difficulty in growth and
4 maintenance of these cells in an *in vitro* culture[10]. The majority of AML cells usually
5 undergo spontaneous apoptosis and only a subpopulation of the cells proliferate during *in*
6 *vitro* culture[11]. The proliferation and survival of the AML cells increases in the presence of
7 hematopoietic growth factors, co-culture with stromal cells and a 3-dimensional
8 environment[10-12]. It has also been shown that AML cells have reduced sensitivity to
9 chemotherapeutic agents in 3D cultures[13]. Insufficient information on molecular interaction
10 between the AML LSCs and their microenvironment is one of the main reasons for failure of
11 current therapeutic approaches[14]. The new approaches should be focused on selectively
12 inhibiting LSC by disrupting the interaction between them and their niche environment but at
13 the same time preserving the normal haematopoiesis. Long term low level *BCR-ABL*
14 oncogene detection by sensitive PCR techniques in CML patients who achieve major
15 molecular response to tyrosine kinase inhibitors is believed to be due to the survival of LSC
16 in the BM niches in spite of the inhibition of BCR-ABL kinase activity[15].

17
18
19
20
21
22
23
24
25
26
27
28
29
30
31
32
33 A 3D culture mimicking BM microenvironment provides a model through which the
34 mechanism of LSC maintenance can be explored and this facilitates the investigations toward
35 developing drugs targeting the survival pathways activated by such interactions. Various 3D
36 cultures have been developed so far for studying leukaemia cells. We have already developed
37 PMMA-HA fibre-based scaffold to show the influence of 3D culture on reduced sensitivity of
38 leukaemia cells to the tested antileukaemia agents[16]. The PMMA-HA scaffold provides a
39 3D structure and by having hydroxyapatite (HA) simulate some characteristics of the bone
40 however, it lacks the spongy structure of the BM. To develop a scaffold with pores similar
41 to bone lacuna we developed in this work, a foam-based scaffold with spongy structure
42 using alginate biomaterial[17, 18]. Microbubble technology was applied to produce the foam
43 with the expected size of the pores[19]. This foam-based 3D culture supported the growth of

1
2
3 normal haematopoietic and also leukaemia cells, and similar to *in vivo* condition it promoted
4 cell differentiation. This system reduced the sensitivity of the leukaemia cells to
5 antileukaemia agents. Due to simulating the physiological condition our foam-based scaffold
6 can be used for drug sensitivity studies of the primary leukaemia cells.
7
8
9
10

11 12 **2.Results**

13 14 **2.1. Material and solution characteristics**

15
16 In the process of microbubble production using a microfluidic technique, parameters such as
17 gas pressure, liquid flow rate and viscosity have a significant influence on the diameter size
18 of the bubble and their formation in the V-junction device (Figure S1a). Monodisperse
19 microbubbles with average diameter 150 μ m were obtained at gas pressure of 95-120 kPa and
20 obtain flow rate of 200-250 μ l/min. In this study to improve the stability of alginate
21 microbubbles, they were collected in 2% wt. calcium chloride solution to cross-link the
22 bubbles shell. This made the shell stronger and as a result the bubbles lasted longer and
23 allowed time for the foam structure to evolve (Figure S1b). Physical properties such as
24 viscosity and surface tension have significant impact on the bubble formation process. In the
25 current study, the surface tension of alginate-PEG liquid was measured to be 49 mN/m, using
26 a Kruss Tensiometer (Model-K9, Kruss GmbH, Germany). The viscosity was measured to be
27 20 mPa s, using a Brookfield DV-11 Ultra programmable Rheometer (Brookfield
28 Engineering Laboratory Inc., Middleboro, MA, USA). To obtain accurate results different
29 measurements were performed at ambient temperature (22 °C) and the average of seven
30 readings was taken to ensure accuracy.
31
32
33
34
35
36
37
38
39
40
41
42
43
44
45
46
47
48
49
50

51 52 **2.2. Foam-based scaffold**

53
54 Foams are metastable inclusions of gas in a fluid phase and are frequently used in the food
55 industry and biomedical applications. In this study, solid foam structures with high porosity
56
57
58
59
60

1
2
3 were successfully prepared by cross-linking the alginate microbubbles (Fig 1). The foam
4 scaffold was dried (as observed by optical microscopy) after 10 days of incubation in a
5 desiccator. Foam scaffolds showed typical ladder-like porous structure with porous size
6 ranging between 20 and 200 μm (Figure 1).
7
8
9
10

11 12 **2.3. Bioactivity and biocompatibility of scaffold**

13
14
15 To allow cell growth and support biocompatibility features, it is critical that the scaffolds
16 have high porosity and bioactive nanoparticles are incorporated in them. Hydroxyapatite
17 (HA) is the main inorganic component of bone material and is widely used in various
18 biomedical applications due to its excellent bioactivity and biocompatibility. In this study to
19 support cell compatibility, HA nanoparticles (diameter < 200 nm, 5% wt.) were added to the
20 scaffold structure. This was achieved by adding the HA to the alginate solution prior to
21 forming bubbles using the v-junction. We observed settlement of K562 and primary AML
22 cells in the microcavities of the scaffold which is an evidence for the biocompatibility of the
23 prepared foams (Figure 2). The cells were concentrated in the microcavities and around the
24 scaffolds indicating the attraction of this scaffold to the leukaemia cells.
25
26
27
28
29
30
31
32
33
34
35
36
37

38 **2.4. Differentiation of the primary haematopoietic cells and acute myeloid leukaemia cells**

39
40 Mononuclear cells from a newly diagnosed AML patient were cultured in the presence and
41 absence of scaffold (in triplicate). The cell counts after 5 days of culture showed larger
42 number of AML cells in the scaffold compared to no scaffold (Figure S2) this supported the
43 cell friendly nature of the alginate scaffold. To investigate whether the scaffolds influence the
44 differentiation of the leukaemia and normal stem/progenitors, the myeloid differentiation of
45 the CD34⁺ cells from one normal and two AML patients were investigated in the presence or
46 absence of foam scaffolds for 3 days. The antigenic expression of primary normal
47 haematopoietic cells (Figure 3A) and two different acute myeloid leukaemia cells (Figure 3B
48
49
50
51
52
53
54
55
56
57
58
59
60

1
2
3 and 3C) from day 0 to 3 was measured by flowcytometry. Normal CD34⁺ precursors showed
4 stronger and more homogenous expression of the myeloid associated antigens CD117 and
5 CD13 after 3 days culture in the foam-based scaffold compared to non-scaffold (2D) culture
6 indicating enhanced differentiation. Similarly, in figure 3B, myeloblasts had augmented
7 intensity of HLA-DR and CD13. This was even more evident in figure 3C, where the blasts
8 showed a profound monocytic differentiation compared to 2D culture, having stronger
9 expression of HLA-DR and CD11b. Enhanced differentiation of CD34⁺ cells to more
10 differentiated cells (represented as reduced CD34⁺ expression) was also observed in
11 myeloblasts from the third AML patient (Figure S3). The findings from this observation
12 suggest that foam-based 3D culture enhances myeloid differentiation in the normal CD34⁺
13 cells and also myeloblasts from AML patients. Further information on the expression of the
14 markers for patients in figure 3 is provided in supplementary information (Table S1 and
15 figure S4).

2.5. Resistance of the CML and AML cells to inhibitory effect of the drugs

31
32
33 Using different types of scaffolds, we showed previously[16] that 3D cultures reduced the
34 sensitivity of leukaemia cell lines to antileukaemia agents. Due to lack of prior knowledge
35 about the potential level of resistance which might be induced by the foam scaffold, we
36 investigated various inhibitory concentration of imatinib or doxorubicin for K562 or HL60
37 and HS-5 cells. In our earlier work, we determined the lowest inhibitory dose of imatinib for
38 K562 to be 0.5 μ M[16]. To determine the lowest inhibitory dose of doxorubicin for HL60
39 cells which is not toxic to HS-5 stromal cells, both cell lines were treated with various doses
40 of doxorubicin followed by MTS assay. This experiment identified 0.1 μ M as the lowest
41 inhibitory dose of doxorubicin for HL60 which had no inhibitory effect on HS-5 cell co-
42 culture (Figure 4). To investigate the potential drug-resistance mediated by the foam-based
43
44
45
46
47
48
49
50
51
52
53
54
55
56
57
58
59
60

1
2 scaffold, K562 and HL60 cells were treated with imatinib and doxorubicin, respectively.
3
4 Treatment of K562 or HL60 cells in foam-based 3D culture reduced their sensitivity to
5
6 imatinib or doxorubicin, respectively (Figure 5 a, b). As stroma is an important component of
7
8 BM microenvironment, to assess the sensitivity of leukaemia cells to antileukaemia agents in
9
10 the context of stromal cells, BM-derived HS-5 stromal cells were seeded to the foam-based
11
12 scaffold. For HL60 cells, addition of HS-5 cells further reduced the sensitivity of HL60 to
13
14 0.1 μ M doxorubicin (Figure 5b). Although addition of HS-5 cells to foam scaffolds increased
15
16 the trend toward resistance, K562 cells treated with 0.5 or 1 μ M imatinib, the difference was
17
18 insignificant (Figure 5a). The lack of any trend toward resistance in the co-culture of HL60
19
20 and HS-5 in foam-based scaffold compared to no HS-5 condition might be due to inhibitory
21
22 dose of doxorubicin on HS-5 at doses higher than 0.1 μ M doxorubicin (Figure 5b). To show
23
24 primary leukaemia cells behave similarly, primary myeloblasts from an AML patient were
25
26 cultured in the presence or absence of foam-based scaffolds and treated with or without
27
28 doxorubicin (0.1, 0.2 and 0.4 μ M) followed by cell proliferation and viability using MTS
29
30 assay at 72 hours. Foam-scaffolds reduced the sensitivity of AML cells to doxorubicin at 0.2
31
32 and 0.4 μ M (Figure 5c). The lack of difference at 0.1 μ M seems to be the lower sensitivity of
33
34 primary AML cells to doxorubicin compared to HL60 cells.
35
36
37
38
39
40

41 **3.Discussion**

42
43 Tissue engineering scaffolds play an important role in biomedical applications by acting as a
44
45 temporary tissue construct or building block for cell accommodation, proliferation and
46
47 differential function[20]. In the current study foam scaffolds were prepared by a microfluidic
48
49 bubbling technique. To overcome the poor stability of the microbubbles which is a limitation
50
51 of this technique crosslinking by calcium chloride was practiced [21]. To improve
52
53 biocompatibility of the scaffold, porous foam was fabricated from natural polymer alginate.
54
55
56
57
58
59
60

1
2
3 To improve cell seeding and growth recently many attempts have been made such as coating
4 the scaffolds with different proteins like collagen and FBS[22-24], here we used HA
5 nanoparticles to make the scaffold more similar to bone marrow microenvironment for
6 biological investigations.
7
8
9

10
11
12 To develop a bone marrow like environment with niche like structures we formed foam-
13 based scaffolds derived from microbubbles. Application of this technology has the advantage
14 of controlling the size of the microbubbles and as a result controlling the size of the
15 microcavities in the foam. This enabled production of scaffold with pores of about 200 μ m in
16 diameter, which is close in size to the microcavities in the bone [25, 26]. The challenge for
17 using this technology to produce foamed scaffolds is the instability of the produced bubbles
18 which results in destruction of bubbles before forming solid foam during drying. To
19 overcome this problem, we collected microbubbles in calcium chloride solution which caused
20 cross links in the microbubble shell and the formation of solid foam following drying. The
21 images from these scaffolds showed the production of desired microcavities and validates the
22 use of this approach for production of foam-based scaffold.
23
24
25
26
27
28
29
30
31
32
33
34
35
36

37 One of the main purposes of developing artificial bone marrow like structures for culturing
38 leukaemia cells is drug sensitivities[27]. Foam-based 3D culture similar to fiber scaffolds[16]
39 increased the resistance of the leukaemia cell lines to inhibitory effects of imatinib and
40 doxorubicin. Different applied materials in the structure of the fiber and foam-based scaffolds
41 and observation of similar phenotypes in K562 and HL60 cells in response to imatinib and
42 doxorubicin suggest the 3D environment and interaction of the leukaemia cells at different
43 spatial positions has an important influence on their survival and activated signaling
44 pathways, and as a result response to antileukaemia drugs. It has been shown before that 3D
45 cultures influence the cell phenotype and their gene expression compared to 2D environment
46
47
48
49
50
51
52
53
54
55
56
57
58
59
60

1
2
3 [28]. This altered phenotype might be due to activation of another signaling pathway which is
4 targeted by the inhibitor. The other possibility is the altered oxygen concentration in 3D
5 compared to 2D culture. Hypoxia is an important component of the BM niche and contributes
6 to the maintenance of AML cells[29, 30] and also selects bortezomib-resistant CML stem
7 cells[31]. It has been shown that 3D-cultures are better than 2D-cultures in simulating
8 important tumor characteristics *in vivo* such as hypoxia and resulting drug resistant
9 phenotype[32]. The mechanism of resistance might also be due to poor access of drugs to the
10 cells hidden in the niche like spaces in the scaffold. These provide more evidence for the
11 application of 3D culture for drug sensitivity studies. Conventional 2D cultures have been
12 proven to be an unreliable drug development model for prediction of *in vivo* drug efficacy
13 and toxicity[33]. Creating a third dimension for cell culture is clearly more relevant and has
14 to be considered as a practical alternative[34].
15
16
17
18
19
20
21
22
23
24
25
26
27
28
29

30 Our data showed enhanced myeloid differentiation in both normal progenitor and AML
31 myeloblasts in 3D foam-based culture. 3D cultures have also been reported in other studies to
32 be capable of inducing differentiation of the hematopoietic stem cells compared to 2D
33 cultures[35, 36]. 3D cultures mimic an environment to *in vivo* bone marrow niches compared
34 to 2D inducing cell differentiation[37]. Although this observation does not address directly
35 how this can influence resistance to therapeutic agents it might suggest that 3D culture causes
36 higher resistance to antileukaemia agents compared to 2D cultures by inducing higher
37 differentiation rate and production of the more mature cells which are less sensitive to
38 inhibitory effect of antileukaemia agents. As resistance or relapse in AML is considered to be
39 mainly due to the role of LSC, future investigations should aim at measuring the impact of
40 3D cultures on LSCs and if 3D culture affects the self-renewal activity of LSCs. In summary,
41 the conventional 2D culture is not a highly reliable system for drug sensitivity investigations
42 as the drug sensitivity of leukaemia cells obtained from 2D culture is different from what is
43
44
45
46
47
48
49
50
51
52
53
54
55
56
57
58
59
60

1
2
3 observed *in vivo*[38]. Our foam-based 3D culture reduced the sensitivity of leukaemia cells to
4 antileukaemia agents and further induced the differentiation of the normal and leukaemia
5 cells compared to 2D culture. These differences might be attributed to microcavities
6 mimicking bone marrow niches in foam-based 3D culture. We propose to apply this foam-
7 based 3D culture for drug sensitivity investigations and therapeutic target discoveries.
8
9
10
11
12
13

14 **5. Conclusions**

15
16 Recent developments in understanding the role of bone marrow microenvironment in the
17 formation and progress of various myeloid leukaemia has created a new opportunity for
18 development of novel therapeutic approaches. Targeting the interaction between the
19 leukaemia cells and the microenvironment is expected to eradicate leukaemia cells residing in
20 the bone marrow niches. Mesenchymal stromal cells, osteoblasts and extracellular matrix are
21 among the main components of the bone marrow microenvironment whereby their special 3D
22 organization contributes to the formation of niches. This is a very different structure
23 compared to conventional 2D cultures which have been used extensively for measuring the
24 sensitivity of the leukaemia cells to various antileukaemia agents. Our investigations have
25 shown that a higher level of resistance to antileukaemia agents is induced by 3D culture
26 mimicking bone marrow compared to 2D culture and support the application of 3D culture as
27 the *in vitro* model to investigate the drug sensitivity. This has been achieved by using an
28 alginate foam-based scaffold prepared using microbubbles generated by a microfluidic
29 device.
30
31
32
33
34
35
36
37
38
39
40
41
42
43
44
45
46
47

48 **6. Experimental Section**

49 **6.1. Solution preparation**

50
51 All the polymers in this study were purchased from sigma-Aldrich (Poole UK) unless stated
52 otherwise. To prepare the aqueous alginate solution, 1% wt. sodium alginate powder was
53
54
55
56
57
58
59
60

1
2
3 dissolved in deionized water followed by the addition of 0.5% wt. polyethyleneglycol-40
4
5 (PEG- 40S, Sigma-Aldrich, Poole, UK, density; 1300 kg/m^3) as a surfactant. The mixture
6
7 was stirred using a magnetic stirrer (KIKA, Labor-Technology RCT basic stirrer) for two
8
9 hours to allow for even dispersion of the compounds. 0.5% wt. of Phospholipid
10
11 (hydrogenated powder) was weighed and added to the solution followed by further stirring
12
13 for approximately another 2 hours until a homogenous solution was obtained.
14
15

16 17 **6.2. Microfluidic Process**

18
19 A V-junction microfluidic set-up is illustrated in [figure S1a](#). It was used to generate
20
21 monodisperse microbubbles[19]. The V- junction microfluidic device is fabricated using
22
23 poly(methylmethacrylate) via CNC machining. It consists of three Teflon capillaries with a
24
25 constant inner diameter ($200 \mu\text{m}$). The vertical capillary is connected to a gas cylinder, via a
26
27 digital manometer for controlling the pressure supplied to the junction. The sides deck
28
29 capillaries provide solutions flow and are connected to a syringe via a syringe pump
30
31 (Harvard, PHD 4400). To generate microbubbles, the gas pressure was gradually increased
32
33 until it overcame the surface tension of the supplied alginate solution. The liquid and gas
34
35 from all three capillaries met at the intersection zone of the junction. This produced bubbles
36
37 at the gas–liquid interface from the bottom inlet. The bubbles were deposited into arrays
38
39 which dried naturally to give the foam samples. The temperature and relative humidity during
40
41 processing was $21 \text{ }^\circ\text{C}$ and 40 to 60 % respectively.
42
43
44
45

46 47 **6.3. Foam sample analysis**

48
49 The microbubbles size and uniformity were examined using an optical microscope (Zeiss
50
51 Axiotech) fitted with a Nikon Eclipse ME 600 camera. Foam scaffold morphology was
52
53 assessed using a Jeol JSM-6301F field emission scanning electron microscope (FE-SEM,
54
55 JEOL Ltd., Herts, UK). Prior to imaging examination, the samples were coated with 20nm of
56
57
58
59
60

1
2
3 gold under argon using Quorum Q150T Turbo-Pumped Sputter Coater. All the SEM images
4
5 were taken at an acceleration of voltage of 5kV with a working distance of 15–35 mm. The
6
7 average microbubble diameter was determined by measuring their diameter at ~ 50 points in
8
9 the SEM images using the ImageJ software (Version 3.00).
10

11 12 **6.4. Preparation of Normal Hematopoietic and Acute Myeloid leukaemia cells**

13
14 Mononuclear cells (MNCs) were separated by density centrifugation on Ficoll-Hypaque
15
16 (Nycomed, Zürich, Switzerland) from peripheral blood of newly diagnosed AML and CML
17
18 patients and cryopreserved. Informed signed consent was obtained from the patients for using
19
20 their samples for research. The samples were approved for research under Imperial College
21
22 Tissue Bank ethical approval for myeloid leukaemia research. Prior to use in assays, fresh or
23
24 frozen CD34⁺ cells were cultured in StemSpan SFEM supplemented with cytokines (CC100;
25
26 StemCell Technologies) for 24-48 h at 37°C. The donor gave informed consent for research
27
28 application of the sample.
29
30
31
32

33 **6.5. Cell culture**

34
35 For 2D culture, K562, AR230 and HL60 cell lines were cultured in RPMI medium
36
37 supplemented with 10% FBS, 2 mM L-glutamine and 100 U/mL penicillin/streptomycin
38
39 (RF10). The cells were cultured at a concentration of 25e4/ml. For 3D culture, the prepared
40
41 scaffolds were transferred to 24-well culture plates and sterilized by exposure to ultraviolet
42
43 light for 2 hours followed by washing three times with PBS. After the third wash, 1 ml of
44
45 RF10 was added to each well followed by incubation of the plates at 37 °C in a cell culture
46
47 incubator for 24h. Subsequently, the medium was removed. Primary AML cells, K562 or
48
49 HL60 cell lines were suspended at 25 x 10⁴/ml concentration and then 1ml of the cell
50
51 suspension was added to each well. For the drug sensitivity study, a final concentration of
52
53
54
55
56
57
58
59
60

1
2
3 0.5, 1 or 2 μM imatinib or 0.1, 0.2 or 0.4 μM doxorubicin was used. The experiments were
4
5 done in triplicate for the control and treated condition and were carried out twice.
6
7

8 **6.6. Co-culture of HS-5 with Leukaemia cells**

9

10 Foam-based 3D culture was developed by adding HS-5 cells to calcium alginate foam
11 scaffolds. 15×10^4 GFP⁺HS-5 cells were suspended in 1ml RF10 and transferred to each well
12
13 of the plates containing the scaffold foam. 24 hours later 5×10^5 K562 or HL60 cells were
14
15 added to each well. After another 24 hours, the drug treated groups were given 0.5 or 1 μM
16
17 imatinib or 0.1 or 0.2 μM Doxorubicin. 72 hours later, the live K562 or HL60 cells were
18
19 counted using Countess II FL (Life technologies, USA). Each condition was done in triplicate
20
21 and the experiment was done twice. Similar approach was applied to primary AML cells.
22
23
24
25
26

27 **6.7. Differentiation of the cells using Flowcytometry**

28

29 CD34⁺ cells from one normal and two AML patients were cultured in StemSpan
30 (Thermofisher) supplemented with CC100 (StemCell Technologies) in foam-based 3D and
31
32 2D culture. Myeloid markers were measured at the time of culture and then re-assessed after
33
34 3 days. To retrieve the cells, the supernatant was removed from the 3D culture followed by
35
36 washing the scaffold with PBS and then treating the scaffold with Trypsin-EDTA (Sigma-
37
38 Aldrich). After 5 minutes of incubation at 37°C the supernatant was removed and passed
39
40 through filter. Immunophenotype was determined using 8-color Euroflow AML/MDS
41
42 antibody panel tube 1 (CD16 FITC, CD13 PE, CD34 PerCP-Cy5.5, CD117 PE-Cy7, CD11b
43
44 APC, CD10 APC-H7, HLA-DR V450, CD45 V500). Data was acquired in a BD FACSCanto
45
46
47 II flow cytometer (BD) and analysed with Infinicyt software (Cytognos).
48
49
50
51
52

53 **6.8. MTS Assay**

54
55
56
57
58
59
60

1
2
3 Cells (10^4) were suspended in 200 μ L medium \pm inhibitor and cultured in triplicate in a 48-
4 well plate in the presence or absence of inhibitors (imatinib or doxorubicin) at indicated
5 concentrations. Following 72 hours, CellTiter 96 AQueous One Solution MTS Reagent
6 (Promega) was added according to the manufacturer's instructions. 100 μ L of the medium
7 was transferred from each well to 96-well followed by measuring the dye absorbance at 490
8 nm using Multiskan GO Microplate Spectrophotometer (ThermoFisher Scientific).
9
10
11
12
13
14
15
16
17

18 **6.9. Statistical analysis**

19
20 All the statistical analysis was done using Graphpad prism software version 7. A 2-tailed
21 Student *t* test was used for assays with cell lines and primary cells. For 3-(4,5
22 dimethylthiazol-2-yl)-5-(3-carboxymethoxyphenyl)-2-(4-sulfophenyl)-2H-tetrazolium (MTS)
23 assays, 3 independent experiments each with 3 replicates per concentration were performed
24 on unique plates with untreated controls.
25
26
27
28
29
30
31
32

33 **Authors' contributions**

34
35 MK carried out the lab work, participated in data analysis, design the study and drafted the
36 manuscript; EYF, MP participated in data analysis, MO, DC reviewed the data and
37 commented on the manuscript, JSK designed the study, reviewed the data, coordinated the
38 study and helped draft the manuscript, ME, coordinated the study and helped draft the
39 manuscript. All authors gave final approval for publication.
40
41
42
43

44 **Acknowledgment**

45
46 The biological study was supported with fund from *The Friends of Hammersmith Hospital*,
47 *Kay Kendal Leukaemia Fund* and *Leuka*. For the microscopy images, we would like to thank
48 Dr. Tom Gregory for his assistance with SEM imaging.
49
50
51

52 **Conflict of Interest**

53
54 The authors declare no conflict of interest.
55
56
57
58
59
60

References

- [1] Schofield, R. 1978 The relationship between the spleen colony-forming cell and the haemopoietic stem cell. *Blood Cells* **4**, 7-25.
- [2] Fraser, C.C., Eaves, C.J., Szilvassy, S.J. & Humphries, R.K. 1990 Expansion in vitro of retrovirally marked totipotent hematopoietic stem cells. *Blood* **76**, 1071-1076.
- [3] Haylock, D.N., To, L.B., Dowse, T.L., Juttner, C.A. & Simmons, P.J. 1992 Ex vivo expansion and maturation of peripheral blood CD34+ cells into the myeloid lineage. *Blood* **80**, 1405-1412.
- [4] Plaks, V., Kong, N. & Werb, Z. 2015 The cancer stem cell niche: how essential is the niche in regulating stemness of tumor cells? *Cell Stem Cell* **16**, 225-238. (doi:10.1016/j.stem.2015.02.015).
- [5] Di Maggio, N., Piccinini, E., Jaworski, M., Trumpp, A., Wendt, D.J. & Martin, I. 2011 Toward modeling the bone marrow niche using scaffold-based 3D culture systems. *Biomaterials* **32**, 321-329. (doi:10.1016/j.biomaterials.2010.09.041).
- [6] Tan, J., Liu, T., Hou, L., Meng, W., Wang, Y., Zhi, W. & Deng, L. 2010 Maintenance and expansion of hematopoietic stem/progenitor cells in biomimetic osteoblast niche. *Cytotechnology* **62**, 439-448. (doi:10.1007/s10616-010-9297-6).
- [7] Fang, Y. & Eglén, R.M. 2017 Three-Dimensional Cell Cultures in Drug Discovery and Development. *SLAS Discov* **22**, 456-472. (doi:10.1177/1087057117696795).
- [8] Braccini, A., Wendt, D., Jaquier, C., Jakob, M., Heberer, M., Kenins, L., Wodnar-Filipowicz, A., Quarto, R. & Martin, I. 2005 Three-dimensional perfusion culture of human bone marrow cells and generation of osteoinductive grafts. *Stem Cells* **23**, 1066-1072. (doi:10.1634/stemcells.2005-0002).
- [9] Jiang, X.S., Chai, C., Zhang, Y., Zhuo, R.X., Mao, H.Q. & Leong, K.W. 2006 Surface-immobilization of adhesion peptides on substrate for ex vivo expansion of cryopreserved

umbilical cord blood CD34+ cells. *Biomaterials* **27**, 2723-2732.

(doi:10.1016/j.biomaterials.2005.12.001).

[10] Griessinger, E., Anjos-Afonso, F., Pizzitola, I., Rouault-Pierre, K., Vargaftig, J., Taussig, D., Gribben, J., Lassailly, F. & Bonnet, D. 2014 A niche-like culture system allowing the maintenance of primary human acute myeloid leukemia-initiating cells: a new tool to decipher their chemoresistance and self-renewal mechanisms. *Stem Cells Transl Med* **3**, 520-529. (doi:10.5966/sctm.2013-0166).

[11] Bendall, L.J., Daniel, A., Kortlepel, K. & Gottlieb, D.J. 1994 Bone marrow adherent layers inhibit apoptosis of acute myeloid leukemia cells. *Exp Hematol* **22**, 1252-1260.

[12] Stolze, B., Emmendorffer, A., Corbacioglu, S., Konig, A., Welte, K. & Ebell, W. 1995 Effects of bone marrow fibroblasts on the proliferation and differentiation of myeloid leukemic cell lines. *Exp Hematol* **23**, 1378-1387.

[13] Aljittawi, O.S., Li, D., Xiao, Y., Zhang, D., Ramachandran, K., Stehno-Bittel, L., Van Veldhuizen, P., Lin, T.L., Kambhampati, S. & Garimella, R. 2014 A novel three-dimensional stromal-based model for in vitro chemotherapy sensitivity testing of leukemia cells. *Leuk Lymphoma* **55**, 378-391. (doi:10.3109/10428194.2013.793323).

[14] Tabe, Y. & Konopleva, M. 2015 Role of Microenvironment in Resistance to Therapy in AML. *Curr Hematol Malig Rep* **10**, 96-103. (doi:10.1007/s11899-015-0253-6).

[15] Bhatia, R., Holtz, M., Niu, N., Gray, R., Snyder, D.S., Sawyers, C.L., Arber, D.A., Slovak, M.L. & Forman, S.J. 2003 Persistence of malignant hematopoietic progenitors in chronic myelogenous leukemia patients in complete cytogenetic remission following imatinib mesylate treatment. *Blood* **101**, 4701-4707. (doi:10.1182/blood-2002-09-2780).

[16] Karimpoor, M., E, I.I., Reid, A.G., Claudiani, S., Edirisinghe, M. & Khorashad, J.S. 2017 Development of artificial bone marrow fibre scaffolds to study resistance to anti-leukaemia agents. *Br J Haematol*. (doi:10.1111/bjh.14883).

- 1
2
3 [17] Ahmad, B., Stride, E. & Edirisinghe, M. 2012 Calcium Alginate Foams Prepared by a
4 Microfluidic T-Junction System: Stability and Food Applications. *Food Bioprocess Tech* **5**,
5 2848-2857. (doi:10.1007/s11947-011-0650-3).
6
7
8
9 [18] Elsayed, M., Huang, J. & Edirisinghe, M. 2015 Bioinspired preparation of alginate
10 nanoparticles using microbubble bursting. *Mat Sci Eng C-Mater* **46**, 132-139.
11
12 (doi:10.1016/j.msec.2014.09.036).
13
14
15 [19] Parhizkar, M., Sofokleous, P., Stride, E. & Edirisinghe, M. 2014 Novel preparation of
16 controlled porosity particle/fibre loaded scaffolds using a hybrid micro-fluidic and
17 electrohydrodynamic technique. *Biofabrication* **6**. (doi:Artn 045010
18 10.1088/1758-5082/6/4/045010).
19
20
21
22 [20] Weigelt, B. & Bissell, M.J. 2008 Unraveling the microenvironmental influences on the
23 normal mammary gland and breast cancer. *Semin Cancer Biol* **18**, 311-321.
24
25 (doi:10.1016/j.semcancer.2008.03.013).
26
27
28 [21] Ekemen, Z., Chang, H., Ahmad, Z., Bayram, C., Rong, Z.M., Denkbass, E.B., Stride, E.,
29 Vadgama, P. & Edirisinghe, M. 2011 Fabrication of Biomaterials via Controlled Protein
30 Bubble Generation and Manipulation. *Biomacromolecules* **12**, 4291-4300.
31
32 (doi:10.1021/bm201202y).
33
34
35 [22] Park, H., Radisic, M., Lim, J.O., Chang, B.H. & Vunjak-Novakovic, G. 2005 A novel
36 composite scaffold for cardiac tissue engineering. *In Vitro Cell Dev Biol Anim* **41**, 188-196.
37
38 (doi:10.1290/0411071.1).
39
40
41 [23] Phipps, M.C., Clem, W.C., Catledge, S.A., Xu, Y., Hennessy, K.M., Thomas, V.,
42 Jablonsky, M.J., Chowdhury, S., Stanishevsky, A.V., Vohra, Y.K., et al. 2011 Mesenchymal
43 stem cell responses to bone-mimetic electrospun matrices composed of polycaprolactone,
44 collagen I and nanoparticulate hydroxyapatite. *PLoS One* **6**, e16813.
45
46 (doi:10.1371/journal.pone.0016813).
47
48
49
50
51
52
53
54
55
56
57
58
59
60

- 1
2
3 [24] Nair, A., Thevenot, P., Dey, J., Shen, J.H., Sun, M.W., Yang, J. & Tang, L.P. 2010
4 Novel Polymeric Scaffolds Using Protein Microbubbles as Porogen and Growth Factor
5 Carriers. *Tissue Eng Part C-Me* **16**, 23-32. (doi:10.1089/ten.tec.2009.0094).
6
7
8
9 [25] Lai, X., Price, C., Modla, S., Thompson, W.R., Caplan, J., Kirn-Safran, C.B. & Wang, L.
10 2015 The dependences of osteocyte network on bone compartment, age, and disease. *Bone*
11 *Res* **3**.
12
13
14
15 [26] Nelson, M.R. & Roy, K. 2016 Bone-marrow mimicking biomaterial niches for studying
16 hematopoietic stem and progenitor cells. *J Mater Chem B* **4**, 3490-3503.
17 (doi:10.1039/c5tb02644j).
18
19
20
21 [27] Rodling, L., Schwedhelm, I., Kraus, S., Bieback, K., Hansmann, J. & Lee-Thedieck, C.
22 2017 3D models of the hematopoietic stem cell niche under steady-state and active
23 conditions. *Sci Rep* **7**, 4625. (doi:10.1038/s41598-017-04808-0).
24
25
26
27 [28] Luca, A.C., Mersch, S., Deenen, R., Schmidt, S., Messner, I., Schafer, K.L., Baldus,
28 S.E., Huckenbeck, W., Piekorz, R.P., Knoefel, W.T., et al. 2013 Impact of the 3D
29 microenvironment on phenotype, gene expression, and EGFR inhibition of colorectal cancer
30 cell lines. *PLoS One* **8**, e59689. (doi:10.1371/journal.pone.0059689).
31
32
33
34 [29] Irigoyen, M., Garcia-Ruiz, J.C. & Berra, E. 2017 The hypoxia signalling pathway in
35 haematological malignancies. *Oncotarget* **8**, 36832-36844. (doi:10.18632/oncotarget.15981).
36
37
38
39 [30] Forristal, C.E., Brown, A.L., Helwani, F.M., Winkler, I.G., Nowlan, B., Barbier, V.,
40 Powell, R.J., Engler, G.A., Diakiw, S.M., Zannettino, A.C., et al. 2015 Hypoxia inducible
41 factor (HIF)-2alpha accelerates disease progression in mouse models of leukemia and
42 lymphoma but is not a poor prognosis factor in human AML. *Leukemia* **29**, 2075-2085.
43 (doi:10.1038/leu.2015.102).
44
45
46
47
48
49
50
51
52
53
54
55
56
57
58
59
60

- 1
2
3 [31] Tanturli, M., Giuntoli, S., Barbetti, V., Rovida, E. & Dello Sbarba, P. 2011 Hypoxia
4 selects bortezomib-resistant stem cells of chronic myeloid leukemia. *PLoS One* **6**, e17008.
5 (doi:10.1371/journal.pone.0017008).
6
7
8
9 [32] Imamura, Y., Mukohara, T., Shimono, Y., Funakoshi, Y., Chayahara, N., Toyoda, M.,
10 Kiyota, N., Takao, S., Kono, S., Nakatsura, T., et al. 2015 Comparison of 2D- and 3D-culture
11 models as drug-testing platforms in breast cancer. *Oncol Rep* **33**, 1837-1843.
12 (doi:10.3892/or.2015.3767).
13
14
15 [33] Hutchinson, L. & Kirk, R. 2011 High drug attrition rates--where are we going wrong?
16 *Nat Rev Clin Oncol* **8**, 189-190. (doi:10.1038/nrclinonc.2011.34).
17
18
19 [34] Saleh, F.A. & Genever, P.G. 2011 Turning round: multipotent stromal cells, a three-
20 dimensional revolution? *Cytotherapy* **13**, 903-912. (doi:10.3109/14653249.2011.586998).
21
22
23 [35] Pietrzyk-Nivau, A., Poirault-Chassac, S., Gandrille, S., Derkaoui, S.M., Kauskot, A.,
24 Letourneur, D., Le Visage, C. & Baruch, D. 2015 Three-Dimensional Environment Sustains
25 Hematopoietic Stem Cell Differentiation into Platelet-Producing Megakaryocytes. *PLoS One*
26 **10**, e0136652. (doi:10.1371/journal.pone.0136652).
27
28
29 [36] Liu, H. & Roy, K. 2005 Biomimetic three-dimensional cultures significantly increase
30 hematopoietic differentiation efficacy of embryonic stem cells. *Tissue Eng* **11**, 319-330.
31 (doi:10.1089/ten.2005.11.319).
32
33
34 [37] Sharma, M.B., Limaye, L.S. & Kale, V.P. 2012 Mimicking the functional hematopoietic
35 stem cell niche in vitro: recapitulation of marrow physiology by hydrogel-based three-
36 dimensional cultures of mesenchymal stromal cells. *Haematologica* **97**, 651-660.
37 (doi:10.3324/haematol.2011.050500).
38
39
40 [38] Edmondson, R., Broglie, J.J., Adcock, A.F. & Yang, L. 2014 Three-dimensional cell
41 culture systems and their applications in drug discovery and cell-based biosensors. *Assay*
42 *Drug Dev Technol* **12**, 207-218. (doi:10.1089/adt.2014.573).
43
44
45
46
47
48
49
50
51
52
53
54
55
56
57
58
59
60

Figure captions

Figure 1. (a) SEM image of the foam-based scaffold (yellow arrows indicate pores). (b) Bright dots in the SEM image marked by yellow arrows are HA nanoparticles on the surface of the scaffold. Cross section of the scaffold (c) shows the porous structure and their interconnection. (d) The relative size of the microcavities (pores) is indicated.

Figure 2. Optical microscopy imaging shows the microcavities in the scaffold acting like niches and accommodates (a) K562 and (b) primary AML cells.

Figure 3. The expression of various differentiation markers is shown for one normal control (a) and two AML patients (b and c). In figure (a) CD13 and CD117 markers have increased in 3D compared to 2D and day 0. Figure (b) shows the increased expression of CD13 and HLA-DR in 3D culture compared to 2D and day 0 and increased expression of HLA-DR and CD11b is also observed in 3D compared to 2D and Day 0 in figure (c).

Figure 4. The inhibitory effect of doxorubicin at various doses on HL60 (a) and HS-5 cells (b). The X axis represents various doses of doxorubicin and the Y axis represents the absorbance as measured by Multiskan GO spectrophotometer. *: p value = 0.2, **: p value = 0.0564, ***: p value = 0.0007, ****: p value < 0.0001

Figure 5. The inhibitory effect of imatinib and doxorubicin on leukaemia cell line and primary cells in the presence or absence of foam-scaffold (with or without HS-5) is shown here. (a) shows the percentage of live K562 cells compared to untreated control for each condition 72h after adding 0.5 or 1 μ M imatinib. (b) shows the percentage of live HL60 cells compared to untreated control for each condition 72h after adding 0.1, 0.2 or 0.4 μ M doxorubicin. Figure 6c shows the influence of foam-based scaffold on the inhibition of primary AML cells from a patient. The X axis represents various doses of imatinib (a) or doxorubicin (b, c). The p value higher than 0.05 (not significant) is shown as *.

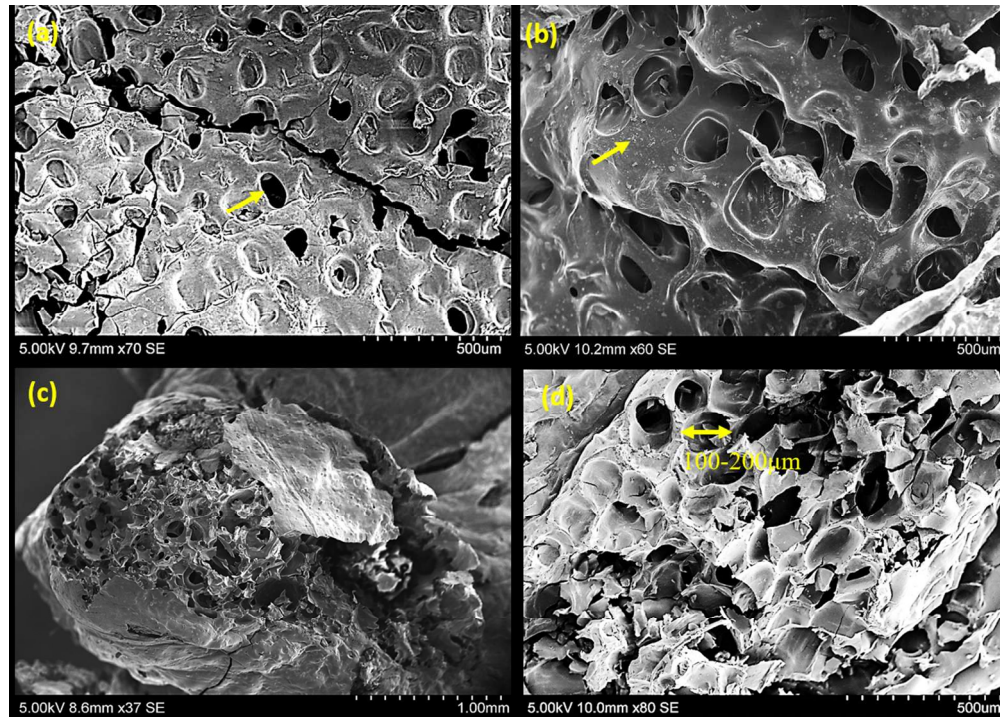


Figure 1. (a) SEM image of the foam-based scaffold (yellow arrows indicate pores). (b) Bright dots in the SEM image marked by yellow arrows are HA nanoparticles on the surface of the scaffold. Cross section of the scaffold (c) shows the porous structure and their interconnection. (d) The relative size of the microcavities (pores) is indicated.

220x157mm (150 x 150 DPI)

1
2
3
4
5
6
7
8
9
10
11
12
13
14
15
16
17
18
19
20
21
22
23
24
25
26
27
28
29
30
31
32
33
34
35
36
37
38
39
40
41
42
43
44
45
46
47
48
49
50
51
52
53
54
55
56
57
58
59
60

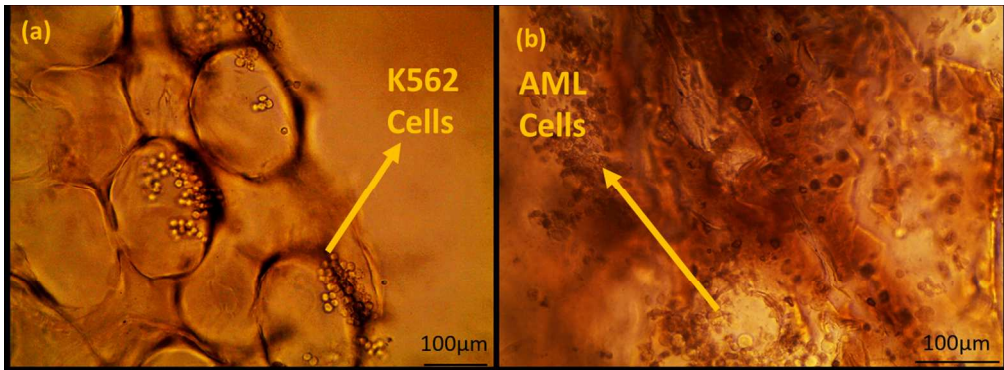


Figure 2. Optical microscopy imaging shows the microcavities in the scaffold acting like niches and accommodates (a) K562 and (b) primary AML cells.

237x87mm (150 x 150 DPI)

Review Only

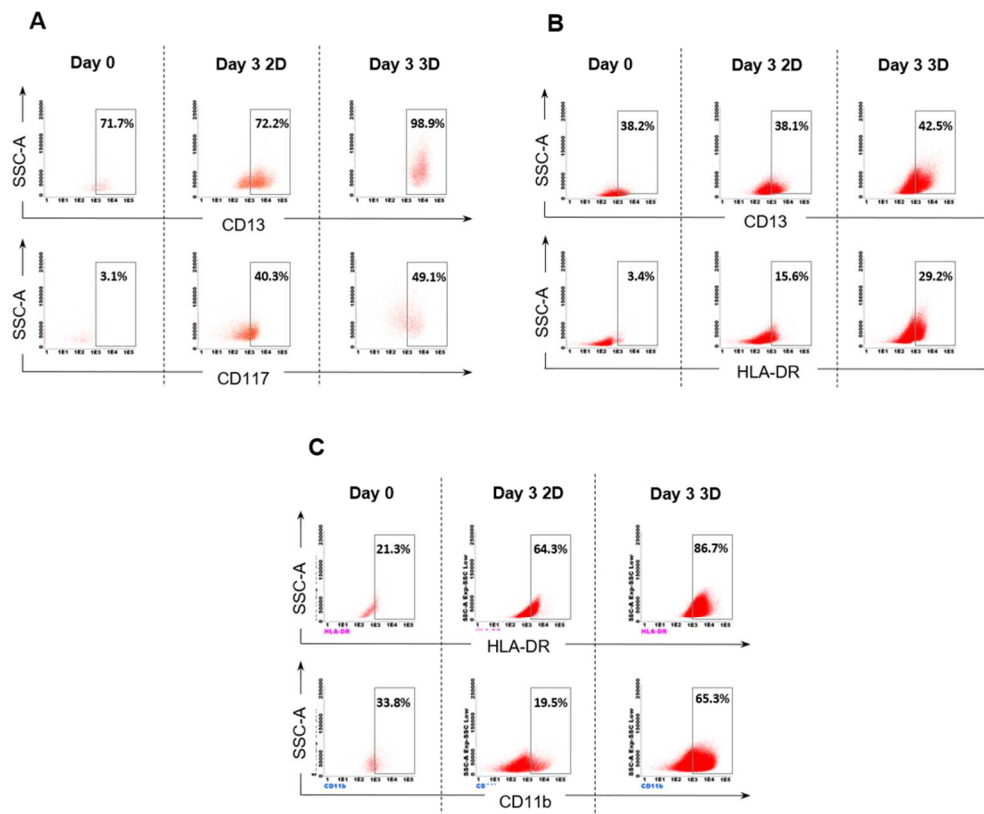


Figure 3. The expression of various differentiation markers is shown for one normal control (a) and two AML patients (b and c). In figure (a) CD13 and CD117 markers have increased in 3D compared to 2D and day 0. Figure (b) shows the increased expression of CD13 and HLA-DR in 3D culture compared to 2D and day 0 and increased expression of HLA-DR and CD11b is also observed in 3D compared to 2D and Day 0 in figure (c).

187x154mm (150 x 150 DPI)

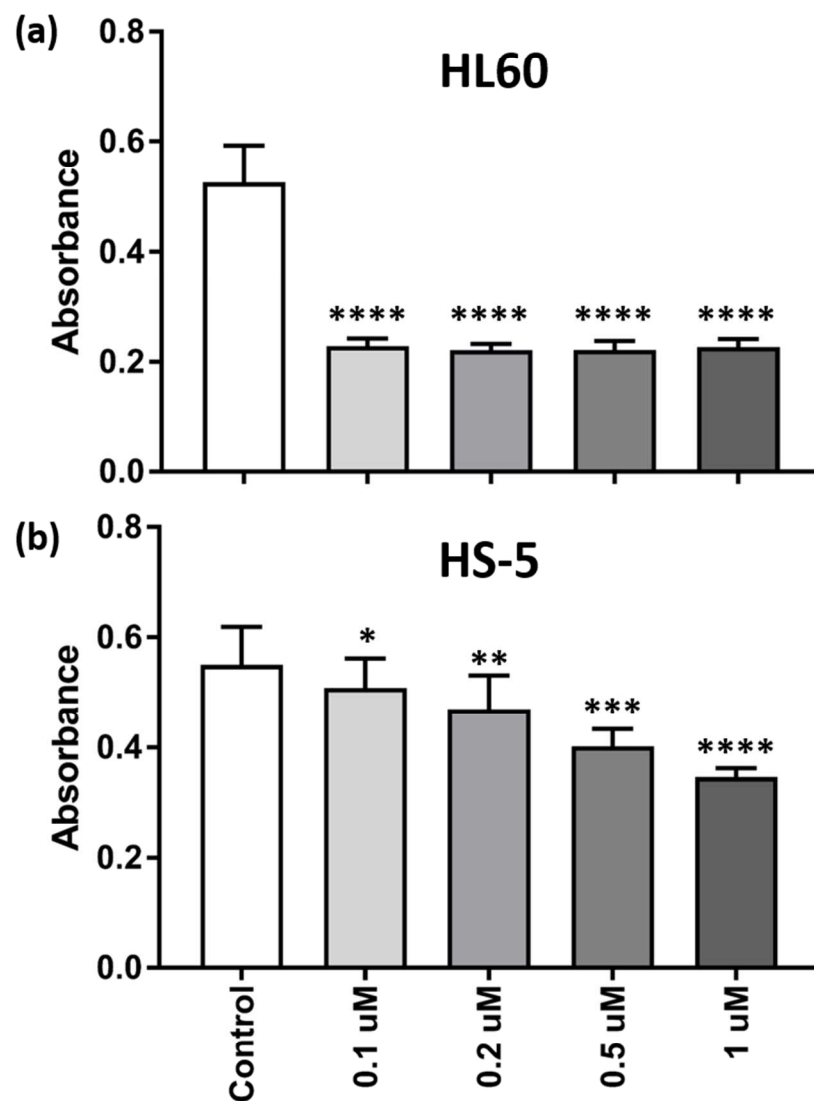


Figure 4. The inhibitory effect of doxorubicin at various doses on HL60 (a) and HS-5 cells (b). The X axis represents various doses of doxorubicin and the Y axis represents the absorbance as measured by Multiskan GO spectrophotometer. *: p value = 0.2, **: p value = 0.0564, ***: p value = 0.0007, ****: p value < 0.0001

221x297mm (96 x 96 DPI)

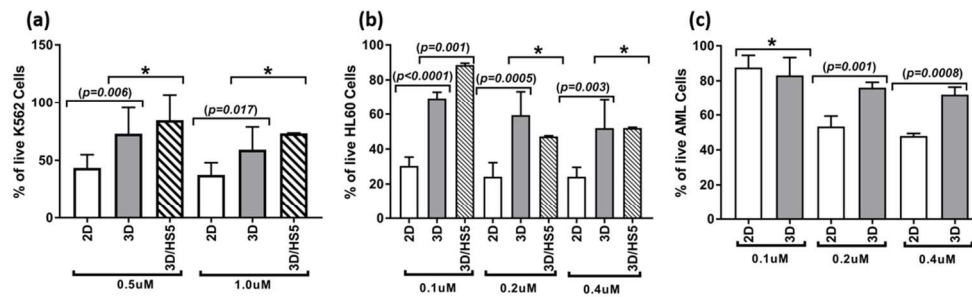


Figure 5. The inhibitory effect of imatinib and doxorubicin on leukaemia cell line and primary cells in the presence or absence of foam-scaffold (with or without HS-5) is shown here. (a) shows the percentage of live K562 cells compared to untreated control for each condition 72h after adding 0.5 or 1 μ M imatinib. (b) shows the percentage of live HL60 cells compared to untreated control for each condition 72h after adding 0.1, 0.2 or 0.4 μ M doxorubicin. Figure 6c shows the influence of foam-based scaffold on the inhibition of primary AML cells from a patient. The X axis represents various doses of imatinib (a) or doxorubicin (b, c). The p value higher than 0.05 (not significant) is shown as *.

338x104mm (96 x 96 DPI)